



Universiteit  
Leiden  
The Netherlands

## Cellular cryo-tomography of nidovirus replication organelles

Wolff, G.

### Citation

Wolff, G. (2022, June 29). *Cellular cryo-tomography of nidovirus replication organelles*. Retrieved from <https://hdl.handle.net/1887/3421526>

Version: Publisher's Version

License: [Licence agreement concerning inclusion of doctoral thesis in the Institutional Repository of the University of Leiden](#)

Downloaded from: <https://hdl.handle.net/1887/3421526>

**Note:** To cite this publication please use the final published version (if applicable).

# CHAPTER 3

## **Mind the gap: Micro-expansion joints drastically decrease the bending of FIB-milled cryo-lamellae**

**Georg Wolff<sup>1</sup>, Ronald W.A.L. Limpens<sup>1</sup>, Shawn Zheng<sup>2</sup>, Eric J. Snijder<sup>3</sup>,  
David A. Agard<sup>2</sup>, Abraham J. Koster<sup>1</sup>, Montserrat Bárcena<sup>1</sup>**

<sup>1</sup>Section Electron Microscopy, Department of Cell and Chemical Biology,  
Leiden University Medical Center, Leiden, The Netherlands.

<sup>2</sup>Department of Biochemistry and Biophysics, Howard Hughes Medical Institute, University of  
California San Francisco, San Francisco, CA 94143, USA.

<sup>3</sup>Molecular Virology Laboratory, Department of Medical Microbiology,  
Leiden University Medical Center, Leiden, The Netherlands.

## Abstract

Cryo-focused ion beam (FIB)-milling of biological samples can be used to generate thin electron-transparent slices from cells grown or deposited on EM grids. These so called cryo-lamellae allow high-resolution structural studies of the natural cellular environment by in situ cryo-electron tomography. However, the cryo-lamella workflow is a low-throughput technique and can easily be hindered by technical issues like the bending of the lamellae during the final cryo-FIB-milling steps. The severity of lamella bending seems to correlate with crinkling of the EM grid support film at cryogenic temperatures, which could generate tensions that may be transferred onto the thin lamella, leading to its bending and breakage. To protect the lamellae from such forces, we milled “micro-expansion joints” alongside the lamellae, creating gaps in the support that can act as physical buffers to safely absorb material motion. We demonstrate that the presence of micro-expansion joints drastically decreases bending of lamellae milled from eukaryotic cells grown and frozen on EM grids. Furthermore, we show that this adaptation does not create additional instabilities that could impede subsequent parts of the cryo-lamella workflow, as we obtained high-quality Volta phase plate tomograms revealing macromolecules in their natural structural context. The minimal additional effort required to implement micro-expansion joints in the cryo-FIB-milling workflow makes them a straightforward solution against cryo-lamella bending to increase the throughput of in situ structural biology studies.



3

MIND THE GAP: MICRO-EXPANSION JOINTS DRASTICALLY DECREASE THE BENDING OF FIB-MILLED CRYO-LAMELLAE

## Introduction

The emergence of focused ion beam (FIB)-milling has opened an exciting and rapidly growing field in cryo-electron microscopy (cryo-EM) by facilitating structural studies in the natural cellular environment. While small biological specimens (e.g. purified macromolecules) can nowadays be studied at near-atomic resolution by cryo-EM (69), the limited penetration depth of the electron beam in a transmission electron microscope (TEM) precludes the direct observation of intracellular structures in thicker samples like eukaryotic cells. To overcome this limitation, a dual-beam scanning-electron-microscope (SEM) equipped with a FIB and a cryo-sample stage, termed cryo-FIB/SEM, can be used to mill an electron-transparent slice from a cell (66, 81). Essentially, any internal region of a cell can be accessed by removing excess material above and below it with a focused beam of gallium ions, resulting in a less than 300 nm thick cryo-lamella that is suitable for *in situ* structural studies of macromolecular complexes by cryo-electron tomography (cryo-ET) (86, 89, 176-179). Although the cell volume accessible by FIB-milling is considerably smaller than that in a cryo-section, a major advantage is that cryo-lamellae do not suffer from the mechanical artefacts (compressions and crevasses) produced in the alternative cryo-ultramicrotomy approach (180).

The FIB-milling workflow to generate lamellae, described in detail in (181, 182), is very similar across different laboratories and studies, with only small variations tailored to the requirements of specific samples. In short, cells grown or deposited on an EM grid are plunge-frozen and transferred to a cryo-stage in a FIB/SEM instrument. Here, a FIB is applied to the sample at shallow angles, using decreasing beam currents as the distance between the milling areas above and below the region of interest is gradually reduced, and the process is monitored by SEM and FIB imaging. The initial higher FIB currents allow the fast removal of bulk material, while low beam currents subsequently ensure a more gentle polishing of the lamella to its final thickness. A layer of organometallic platinum is applied on the sample before milling to further protect the lamellae from unwanted erosion by scattering ions and curtaining (183). Most cryo-lamellae have a width of 10–20  $\mu\text{m}$  and are reproducibly milled to a thickness of 150–300 nm, although special strategies are available as well to produce lamellae below 100 nm thickness, desirable for high resolution reconstructions (184).

Currently, cryo-FIB-milling is still a rather laborious and time-consuming technique: a day of milling will produce about 5–10 lamellae. These lamellae represent only a tiny fraction of the cellular volume and thus, depending on the specific target to be imaged, may or may not contain the feature of interest. Consequently cryo-FIB-milling is a low-throughput technique and every factor hampering the workflow poses a serious obstacle for its successful application. One of these complicating factors that is regularly observed is the bending of cryo-lamellae during the final milling steps. This first becomes obvious in the ion-beam view as an offset of the lamella front edge from the ideal plane defined by the milling pattern (Fig. 1A), which leads to unintended removal of material and thus damage to the lamellae (Fig. 1B) often rendering them unusable for subsequent cryo-ET studies.

While bending usually accounts for a moderate fraction of the total lamellae, in practice it can become a hurdle that is almost impossible to overcome. In particular, we have noticed that the FIB-milling success rate can critically depend on the specific batch of commercial grids commonly used in the field, whose quality is not directly under the control of the researcher. Ideally, the desired grid support should be flat at all temperatures; however, changes in morphology at low temperatures resulting in a “wavy” support film can be observed (Fig. 1C-D). This cryo-criinkling phenomenon was recognized in the early times of cryo-EM (185)

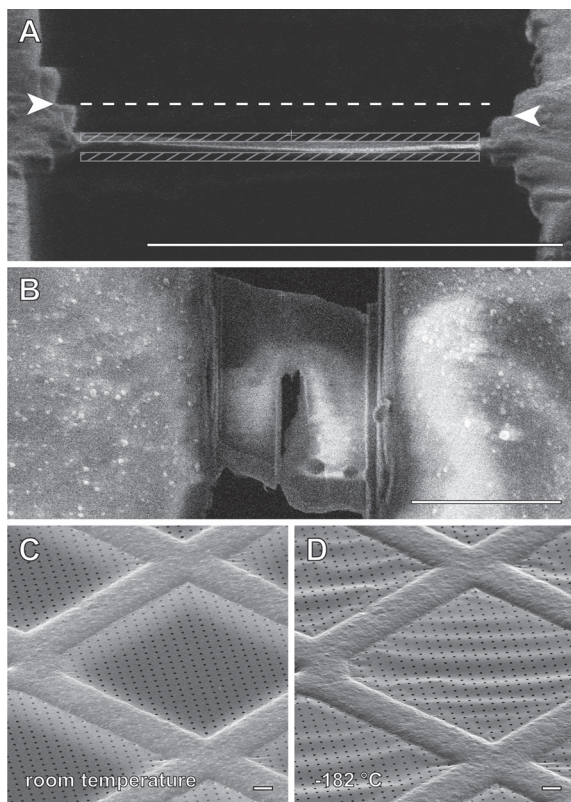


**Figure 1.** Cryo-lamella bending and temperature stability of the support grids. (A) Bending of a cryo-lamella during the final thinning steps of FIB-milling as observed by FIB-imaging from the direction of milling. The offset between the left and right edges of the lamella (white arrowheads) is a clear sign of major sample deformations during milling. The striped grey rectangles represent the milling patterns during the final milling step and define the ideal lamella central plane. Lamella bending becomes recognizable by an offset of any part of the lamella front end to this central plane. (B) Lamella bending leads to unwanted erosion and loss of material in the lamella, as observed by SEM-imaging from top view, which can eventually result in breaking of the lamella. Cryo-lamella bending seems to correlate with the crinkling of the grid support film that occurs during freezing. The grid support film, flat at room-temperature (C) crinkles at cryogenic temperatures (D). Scale bars, 10  $\mu\text{m}$ .

and is primarily caused by the difference in the thermal expansion coefficients between the grid and the support film materials. Therefore, cryo-crinkling of the carbon film on gold grids is a phenomenon that is to be expected. In our experience, the severity of cryo-crinkling can vary between grid batches, which could be due to differences in carbon film thickness, composition or its degree of attachment to the grid. With grid batches with more severe cryo-crinkling, our lamella milling success rate dropped from  $\sim 63\%$  to  $\sim 23\%$ . Following up on this observation, we considered the possibility that cryo-crinkling could be inducing tensions in the sample that may be released onto a cryo-lamella during milling, leading to its bending. We hypothesized that, in this scenario, generating “micro-expansion joints” alongside a lamella could protect it from such forces and thus prevent bending. The concept of expansion joints originates from construction engineering: structures, such as concrete floors, are equipped with gaps to provide a physical buffer that will safely absorb any developing motion. In our case, they are intended to absorb relaxations of the grid support released upon milling, which otherwise would harm the integrity of the cryo-lamella.

## Results

We developed an improved protocol, which includes the milling of lateral micro-expansion joints into the grid support flanking each lamella site (Fig. 2A–D) and reduces lamella bending. The additional milling time is minimal (2–3 min per lamella) as the micro-expansion joints are only  $\sim 1 \mu\text{m}$  wide and are milled with high currents during the first milling step together with the initial rough milling patterns. They cover the same length as the area milled for lamella generation (in our case about  $50 \mu\text{m}$ ) and are at a distance of 3–4  $\mu\text{m}$  from the lamella,

leaving a sufficient amount of cellular material to support the lamella. Once micro-expansion joints are applied, relaxations in the grid support next to them often become apparent (see Fig. S1), pointing towards a release of physical tensions which otherwise probably would have caused lamella bending during thinning. Furthermore, just a single micro-expansion joint can already improve lamella stability in case a milling site is too close to a grid bar. Subsequent milling steps remain unchanged and thus this adaptation can easily be incorporated in any cryo-lamella protocol. In our case, milling of 10  $\mu\text{m}$ -wide lamellae was performed in four steps using FIB currents from 1 nA to 30 pA (see Supplementary material for details), with a final polishing step thinning them to 130–230 nm thickness. Additionally, we used an increased milling angle during initial rough milling ( $16^\circ$  relative to the grid surface) and gradually reduce it to  $11^\circ$  during polishing. Using a higher angle at the initial milling step allows for better visualization and interpretation of the sample topology. Moreover, this seemed to help avoid excessive abrasion of the organometallic platinum on the front end of a cryo-lamella, which in our experience increases with lower milling angles, especially when using higher beam currents.

In order to assess the impact of this adaptation on the overall success rate of the cryo-lamella workflow, we generated a series of lamellae either with or without micro-expansion joints using EM grids from a batch showing the more severe cryo-crianking. We set the limit to

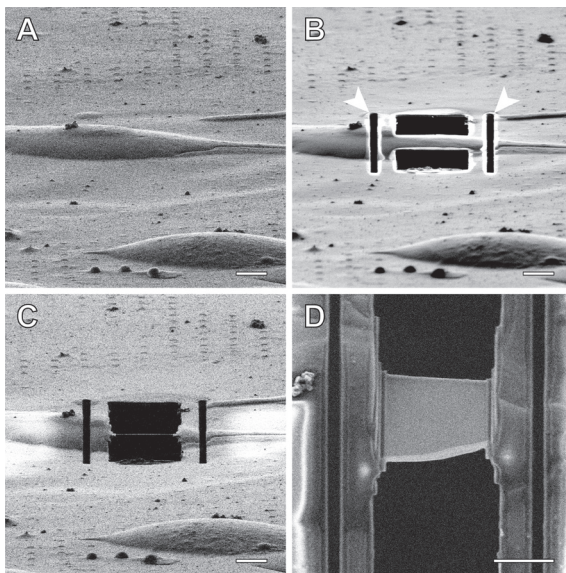
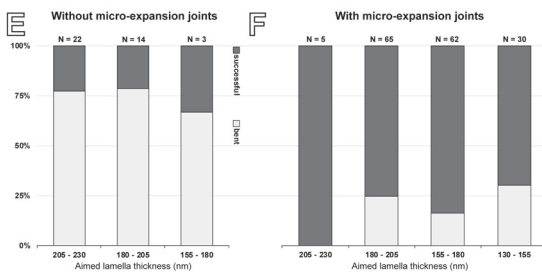


**Figure 2.** Incorporation of micro-expansion joints into the cryo-FIB-milling workflow. (A) First, eukaryotic cells (murine 17clone1 cells in these images) are grown and plunge-frozen on EM grids, and suitable cells for cryo-FIB-milling are selected. (B) Lateral micro-expansion joints (white arrowheads) are generated during the initial rough milling step with higher ion-beam currents (1–0.5 nA) simultaneously to the first milling patterns above and below the region of interest. Micro-expansion joints are generated at a distance of 3–4  $\mu\text{m}$  from the lamella, leaving a sufficient amount of cellular material to support the lamella. (C) Subsequently, the lamella is gradually thinned while reducing the ion-beam currents down to 30 pA during polishing to the final thickness. (A–C) From the ion-beam view the sample morphology and the lamella thickness can be assessed during the process. (D) SEM top-view image of the final lamella showing the typical homogeneous contrast of a thinned and fully intact lamella without signs of bending. Scale bars 5  $\mu\text{m}$ . (E, F) Comparison of the success rates in the milling of all the cryo-lamellae prepared in this study. (E) When micro-expansion joints were not applied to the lamella site, the majority of the lamellae bent during the final milling steps, regardless of the intended thickness (77% bent lamellae in total). (F) Upon addition of micro-expansion joints, 78% of the lamellae could successfully be thinned to their final thickness (as estimated by the distance of the milling patterns during the final milling step) without signs of bending.







categorize a lamella as bent if, during the polishing step, any part of the lamella front edge showed an offset of more than 50 nm from the central plane defined by the milling patterns. It should be noted that more severe cases with much higher offsets can also occur at the previous fine milling step. In both cases the chances are very high that, upon further milling, the bending increases and large parts of the lamella will be damaged. To rule out any influence of variations in quality per grid, we initially milled cryo-lamellae both with and without micro-expansion joints on each grid and could already observe a statistically significant decrease in lamella bending when applying micro-expansion joints. Subsequently we expanded our dataset to a total of 201 lamellae with a thickness ranging from 130 to 230 nm, as estimated by the distance between the applied milling patterns. While for lamellae without micro-expansion joints only 23% could be thinned to their final (desired) thickness without bending, we were able to successfully mill 78% of the lamellae when applying micro-expansion joints (see Fig. 2 E–F). This analysis demonstrated that the addition of micro-expansion joints resulted in a highly significant increase in the success rate of cryo-lamella milling ( $p$ -value  $3.5 \times 10^{-11}$ , chi-square test). Preliminary data with cells grown on gold grids covered with silicon dioxide support films, which have been recently proposed as an alternative to carbon film (186), showed a similar favourable trend in the milling success rate when using micro-expansion joints ( $n=18$  total lamellae,  $p$ -value  $4.5 \times 10^{-3}$ , Fisher's exact test).

While the generation of micro-expansion joints clearly prevented lamella bending, the removal of additional material from the support and the cell that holds the hanging lamella could potentially create instability and conductivity issues affecting other parts of the workflow, namely, transfer and imaging. To explore these concerns, we imaged a major fraction of the cryo-lamellae with micro-expansion joints in a 300 kV TEM (Fig. 3). The transfer of lamellae between instruments is one of the most critical steps in the cryo-lamella workflow, which can easily lead to the destruction of the lamellae. Of the 110 lamellae imaged, 106 did not show any transfer damage while only 3 had a crack and one had been completely destroyed. Therefore, the addition of micro-expansion joints does not seem to reduce the stability of the lamellae during transfer.

To assess whether micro-expansion joints would be limiting the stability and conductivity during TEM imaging, we performed cryo-ET using the Volta phase plate (an imaging mode particularly sensitive to charging effects (86, 187)) on suitable areas containing recognizable cellular features. Our experimental data indicates that micro-expansion joints, even though they interrupt part of the conductive layer between the lamella and the EM grid, do not hamper Volta phase plate imaging as we were able to collect automated tilt-series without visible signs of charging. Nevertheless, a more detailed analysis of the movie frame shifts measured with MotionCor2 (188) indicated that micro-expansion joints may increase beam-induced sample movement. Close to zero degree tilt the maximum frame shifts were similar with and without micro-expansion joints. However, we observed an increase in the frame-to-frame shifts at higher tilt angles in the presence of micro-expansion joints. Specifically, the shift between the first two movie frames at higher tilt angles increased by an average of 1.1–2-fold. Interestingly, the larger shifts occurred exclusively in the direction orthogonal to the tilt axis and tended to increase with the tilt angle. This aligns with the possibility that micro-expansion joints give the lamellae more freedom to move vertically. Though the consequences of this effect appear to be moderate and in most cases will not be a limiting factor, they could be compensated for by increasing the number of frames or, alternatively,

by discarding initial frames (189). In our experimental conditions, the correction provided by the movie-frame alignment step was sufficient to obtain high quality tomograms, in which individual macromolecular structures could be identified (e.g. ATP-synthase complexes embedded in the cristae membranes of mitochondria (190), Fig. 3C–D).

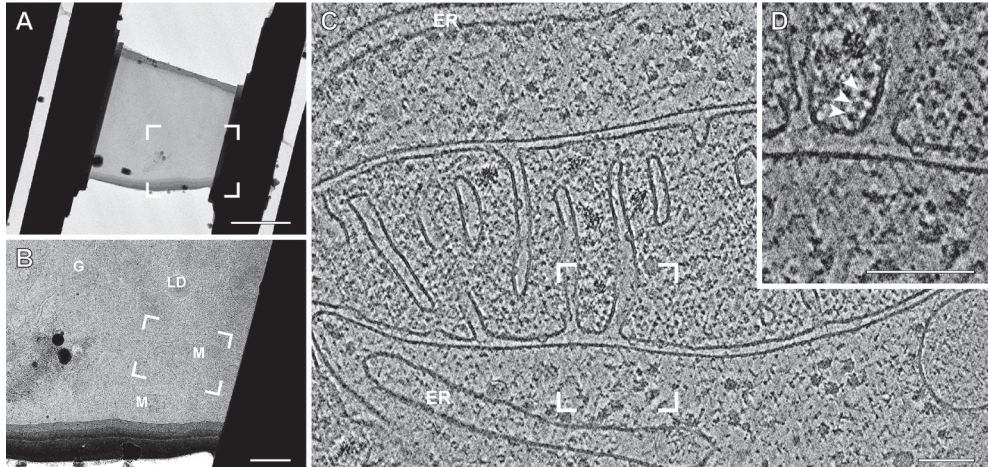


**Figure 3.** TEM imaging and cryo-electron tomography on a lamella milled with micro-expansion joints. (A) A cryo-lamella with micro-expansion joints observed in a 300 kV TEM. The low-resolution overview shows the structural integrity of the lamella. The boxed area indicates the region enlarged for identification of intracellular membranous structures (B), such as the Golgi apparatus (G), lipid droplets (LD) or mitochondria (M). From the selected area of interest (framed in white), a tilt-series was acquired using a Volta phase plate. (C) Slice through a tomogram of this area, reconstructed with AreTomo (see Supplementary material), which shows a mitochondrion, endoplasmic reticulum (ER) membranes and various macromolecules in their structural context. (D) Close-up of the mitochondria highlighting individual ATP-synthase complexes embedded in the cristae membranes (white arrowheads). The thickness of this cryo-lamella was 130 nm, as measured from the tomographic reconstruction. Tomographic data collection was done at  $-0.5\ \mu\text{m}$  defocus and a pixel size of 0.351 nm. Scale bars, 5  $\mu\text{m}$  (A), 1  $\mu\text{m}$  (B) and 100 nm (C, D).

## Discussion

In summary, our results demonstrate a significant improvement in the success rate of cryo-lamella preparation by adding micro-expansion joints to milling sites. Micro-expansion joints do not decrease lamella stability during transfer, and seem to produce only a tolerable increase in beam-induced motion. The effectiveness of this approach strongly supports the notion that tensions in the grid support are present and that they are a major cause for lamella bending, a reoccurring problem in cryo-FIB milling that currently limits the yield of this technique. Whether cryo-krinkling is responsible for these tensions, as our data suggests, remains to be established, as other factors, such as larger scale deformations from sample handling, may be playing an additional or primary role. We showed that it is possible to perform cryo-ET using the Volta phase plate on these lamellae, which poses one of the most demanding ways of cryo-ET (187). With the minimal effort required to include micro-expansion joints in any cryo-lamella protocol, this method can easily increase the FIB-milling throughput thus facilitating cellular cryotomography studies.



## Materials and methods

### Cell culture and vitrification.

R1/4 gold Quantifoil or SiO<sub>2</sub> grids, (200 mesh, Quantifoil Micro Tools, Jena, Germany) were cleaned overnight by placing them on a chloroform soaked filter paper in a sealed glass dish. This chloroform treatment did not affect the cryo-creasing of the support film, as assessed by visual inspection in the cryo-SEM. After letting them dry, the grids were glow-discharged and placed in 3.5 cm diameter cell culture dishes (Greiner Bio-One, Frickenhausen, Germany) containing PBS. After UV-sterilization for 30 min in a laminar-flow, PBS was replaced by cell culture medium containing 100,000 17clone1 or Huh7 cells per dish and incubated at 37 °C overnight. After retrieval of the grids from the cell culture dish using 5/15 style kinked tweezers (Dumont, Montignies, Switzerland), they were transferred to the tweezers of a Leica EM GP (Leica microsystems, Wetzlar, Germany) automated plunge-freezer, and plunge frozen after applying 15 s of blotting from the backside of the grid with chamber conditions of 37 °C and 95% humidity. After being plunge frozen in liquid ethane, the grids were stored in liquid nitrogen until used for cryo-FIB-milling.

### Cryo-FIB-Milling.

Lamella preparation was done in an Aquilos cryo-FIB/SEM (Thermo Fisher Scientific, Hillsboro, OR, USA). First, each grid was sputter-coated with platinum (1 kV, 30 mA, 10 Pa, applied for 10 s) to increase conductivity. Subsequently a layer of organometallic platinum was applied onto the sample by the gas injection system (GIS) operated at 28 °C for 6-7 seconds. Four milling steps (rough, intermediate, fine, polishing) were performed per lamella, for which a 30 kV ion beam was used with 1 to 0.5 nA, 300 to 100 pA, 50 pA and 30 pA probes, respectively. Micro-expansion joints were milled in the initial rough milling step of the lamella using 1 to 0.5 nA currents, simultaneously to the milling of the first patterns above and below the region of interest. The distance between the lamella milling patterns was 3-5 μm during rough milling, 1-1.2 μm during the intermediate step, and 400-500 nm during fine milling. In the rough and intermediate milling the angle was set to 16° and 12°, respectively. During polishing the cryo-lamellae were thinned to 130-230 nm at a FIB angle of 11° relative to the grid surface. After polishing all the lamellae per grid, the sample was sputter-coated with a ~5 nm thick layer platinum (1 kV, 10 mA, 10 Pa, applied for 4 s) with the integrated sputter coater. The process was monitored by FIB and SEM imaging. SEM imaging was done at 3 kV with either a 13 or 25 pA probe with dwell times of 100-500 ns, while FIB imaging was performed at 30 kV using a 10 pA probe with a dwell time of 100 ns.

### Cryo-ET data collection.

Tilt-series acquisition was carried out on a FEI Titan Krios (Thermo Fisher Scientific, Hillsboro, OR, USA) operated at 300 kV and equipped with a Gatan GIF Quantum energy filter (Gatan, Pleasanton, CA). Movie-frames were collected using a Gatan K2 Summit direct detection camera operated in counting mode. The imaging conditions were as follows: EFTEM microprobe, 42,000x magnification, pixel size of 3.51 Å, zero-loss imaging with a 20 eV slit width, beam diameter 3 μm, defocus -0.5 μm. Bi-directional tilt-series acquisition was performed with FEI Tomo4 software, started at 0° with 2° increments and ranged from -50° to +70° stage tilt, to account for the fact that the lamella surfaces were orthogonal to the electron beam at 11°. Volta phase plate was activated before each tilt-series acquisition until the phase shift stabilized at approximately 0.5 pi. The total dose applied on the sample was 140 e<sup>-</sup> per Å<sup>2</sup>, which was distributed over the 61 tilts using a I<sub>0</sub>/I<sub>60</sub> factor of 1.6, resulting in an

average exposure time of 2.8 s per tilt distributed over 14 movie frames.

### Alignment and reconstruction.

After data collection, the movie frames per tilt (14 each) were aligned with MotionCor2 using 5 x 5 patches (188). Tilt-series alignment and tomogram reconstruction were performed with AreTomo. Developed at University of California San Francisco (Zheng and Agard, unpublished) and implemented on a multi-GPU Linux platform, this program fully automates the tomographic workflow from fiducial-free alignment to SART (Simultaneous Algebraic Reconstruction Technique) reconstruction. A typical tomogram can be obtained within a few minutes on a platform with two NVIDIA GeForce GTX 780 Ti GPUs.

### Acknowledgements

We thank Miroslava Schaffer (MPI Martinsried, Germany) for helpful discussions and advice, which inspired this work by drawing our attention to the apparent correlation between cryo-crinkling and lamella bending. We are grateful to Frank Faas (EM section, LUMC, Leiden) for his help in the analysis of MotionCor2 results. High resolution EM data was collected at The Netherlands Centre for Electron Nanoscopy (NeCEN) with assistance from Christoph Diebolder. This work was supported in part by the Howard Hughes Medical Institute and NIH grant R35GM118099 (to DAA and SZ).

### Supplementary figure

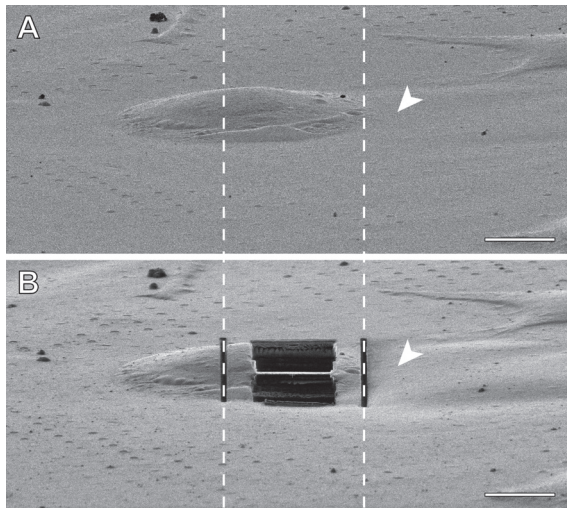


**Figure S1.** Motions in the grid support become apparent upon micro-expansion joint milling. (A) An eukaryotic cell (murine 17clone1 cell) grown and plunge-frozen on an EM grid is selected for cryo-lamella FIB-milling. (B) Upon milling, motion in the support film next to one of the micro-expansion joints becomes apparent (white arrowheads). These deformations are probably caused by tensions in the grid support, that otherwise could have harmed the integrity of the lamella. Scale bars 10  $\mu\text{m}$ .



